Int. J. Electrochem. Sci., 15 **(2020)** 8786 – 8796, doi: 10.20964/2020.09.43

International Journal of
ELECTROCHEMICAL
SCIENCE
www.electrochemsci.org

Imidazoline Gemini Surfactants as Corrosion inhibitor for Copper in NaCl Solution

Zhuang Wenchang[1,a], *Wang Xiqiu*[1,2,*,a], *Luo Xinze*[2,*], *Jia Zhitai*[3,*], *Ma Yalei*[1], *Yu Xiaohu*[1], *Pan Hanqing*[1]

[1] School of Chemistry and Chemical Engineering, Xuzhou Institute of Technology, Xuzhou 221018, P.R. China;
[2] School of Chemistry and Environmental Sciences, Yili Normal University, Yili 835000, P.R. China;
[3] State Key Laboratory of Crystal Materials & Key Laboratory of Functional Crystal Materials and Device, Shandong University, Jinan 250100, China
[*]E-mail: windchant@xzit.edu.cn; luo-xinze@163.com; z.jia@sdu.edu.cn
[a]Contributed to the work equally and should be regarded as co-first authors

Received: 13 March 2020 / *Accepted:* 26 June 2020 / *Published:* 10 August 2020

The Gemini imidazoline surfactants were synthesized from a series of saturated fatty acids.Their corrosion inhibition on copper in NaCl solution was studied by electrochemical method.It was found that the suppressive efficiency depended on pH, carbon chain length, and the concentrations of surfactants. The results show that such kind of surfactants has outstanding suppressive effect on copper in NaCl solution, and the restrained efficiency of Gemini imidazoline in alkaline solution is better than in neutral solution. The shorter the carbon chain length is, the higher the suppressive efficiency is. The higher the concentration of Gemini imidazoline surfactant is, the better the inhibitive effect is.

Keywords: Gemini, imidazoline; surfactants; NaCl solution; inhibition

1. INTRODUCTION

In recent years, the application of Gemini surfactants has gradually expanded. Gemini imidazoline surfactants （GIS）have attracted much attention due to their excellent properties. The GIS is a new type of surfactant developed. GIS, is composed of two surfactant monomers connected by a binding group. The length of two end carbon chains of the monomer may be different [1-4]. Traditional surfactant molecules are usually single-chain structures, and the electrostatic repulsion between hydrophilic groups makes the arrangement of molecules on the interface not close enough, so the interfacial activity of these structures is very low, making their effect poor. Gemini surfactants have

excellent properties because of their special molecular structure. The involvement of bonding groups is the key factor to change the structural diversity of Gemini surfactants, thus affecting the properties of solution and interface[5]. Compared with traditional surfactants, it has very low CMC value, higher solubility, lower Krafft point, special aggregation behavior and better synergistic effect [6-9]. Migahed et al.[10] studied the effect of different ligands on inhibition. It was found that the smaller the ligand, the better the inhibition effect. Yang et al.[11] studied the relationship between the inhibition effect and temperature, and proposed that the inhibition effect increases with the increase of temperature. Tian and Cheng[12] developed two kinds of Imidazoline Corrosion Inhibitors with multi-functional groups by electrochemical test, surface characterization and scanning vibration electrode technology, and studied their corrosion inhibition performance on X65 pipeline steel in formation water of saturated CO_2 oil field. The results show that it has good corrosion inhibition effect. Feng[13] et al. Tested the corrosion inhibition performance of GIS in HCl solution. The results show that at low concentration, the length of carbon chain has little effect on the corrosion inhibition.Yang[14] compared the corrosion resistance of imidazoline monomers with that of GIS. The results showed that the inhibition effect of GIS was better. However, the suppressive efficiency of GIS with different carbon chain lengths have not been reported[15,16].

In the present work, the most suitable pH of the environment for GIS to exert inhibitive effect was explored. At the same time, the influence of structure and concentration of GIS on its suppressive effect was also investigated. A series of imidazoline quaternary ammonium cationic Gemini surfactants were synthesized from fatty acids, diethylenetriamine (DETA) and modifier 1,3-dibromopropane, and their potential polarization curves and electrochemical impedance was measured. The restrained effect of imidazoline surfactant monomer and Gemini surfactant on copper was studied in NaCl solution. The corrosion inhibition performance of GIS in NaCl solution was studied by changing the solution pH, the length of carbon chain and the concentration of inhibitor. The restrained efficiency of GIS on copper in NaCl solution was evaluated.

2. EXPERIMENTAL METHOD

2.1 Materials and Main instruments

2.1.1 Materials

Saturated fatty acids with different carbon chain length (Stearic acid, Plamitic acid, Myristic acid, Lauric acid and Oleic acid)、Diethylenetriamine (DETA), xylene, zinc power, dimethyl-carbonate, 1,3-dibromopropane, acetone, all these reagents are analytical reagent (AR)

2.1.2 Main instruments

ALPHA FT-IR, NMR spectrometer, Electrochemical workstation (CHI600E), motor agitator, Digital display constant temperature oil bath pot

2.2 Synthetic methodology

The synthesis of GIS was carried out with fatty acids with different carbon chain lengths, the synthesis route of GIS was shown in Figure 1.

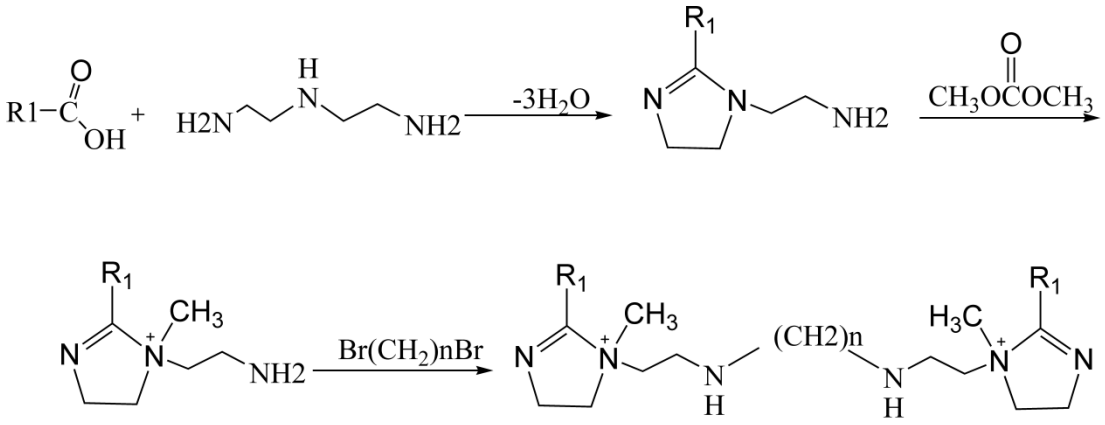

Figure 1. Synthesis route

The product is khaki solid, which is Gemini imidazolinium surfactants. The sysnetic GIS were measured by ALPHA FT-IR and NMR spectrometer. The specific process is shown in Fig.1. FTIR spectra of synthesized cationic GIS are given in Figure 2. ^{1}H-NMR spectra of synthesized Cationic GIS are given in Figure 3. (LG, MG, PG and SG are the GIS based on lauric acid, myristic acid, palmitic acid and stearic acid, respectively[16]. LG is 1,3-di(1-methyl-1-ethylamino-2-n-undecyl-4,5-dihydro-imidazoline) propane, MG is 1,3-di(1-methyl-1-ethylamino-2-n-tridecyl-4,5-dihydro-imidazoline) propane, PG is 1,3-di(1-methyl-1-ethylamino-2-n-pentadecyl-4,5-dihydro-imidazoline) propane, SG is 1,3-di(1-methyl-1-ethylamino-2-n-heptadecyl-4,5-dihydro-imidazoline) propane.)

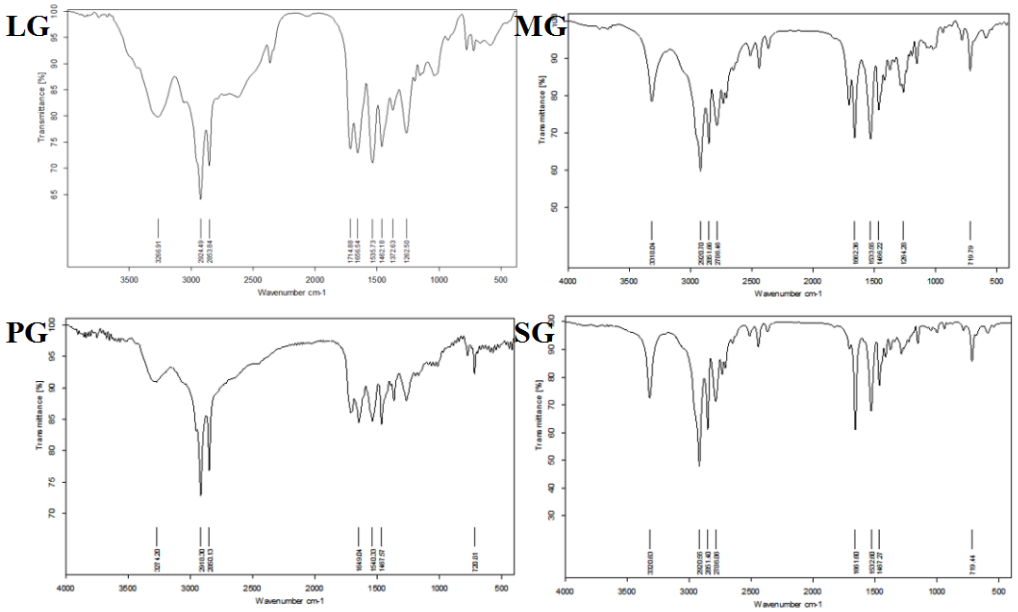

Figure 2. FT-IR spectrum of the GIS.

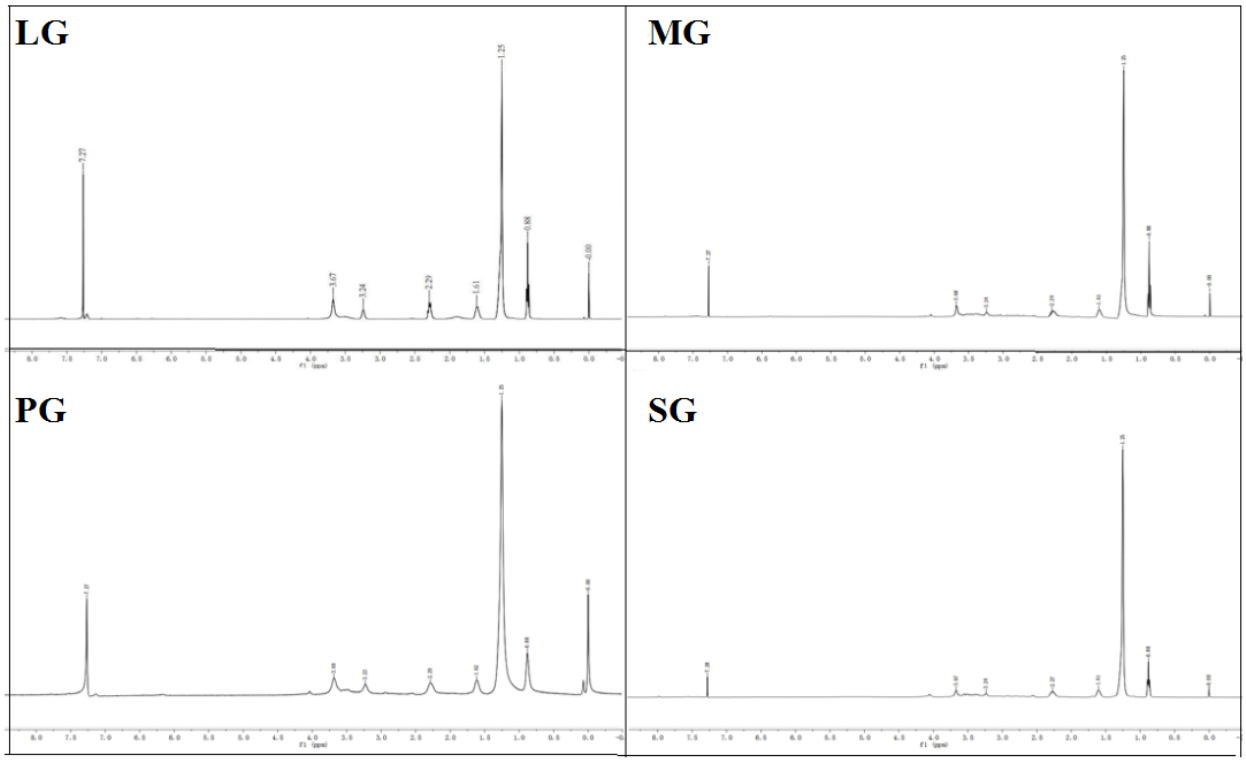

Figure 3. ^{1}H-NMR spectrum of the GIS.

In the Figure 2, FT-IR-Peaks at 1650~1665cm-1 confirmed the preparation of the imidazoline ring. The peaks at 2920~2700cm^{-1} are saturated —CH bonds. Presence of peaks at 730~760cm^{-1} confirms the quaternization of ring. And peaks at 3320~3275cm-1 correspond to NH str- of amide linkage.

In the Figure 3, ^{1}H-NMR-peaks at 7.27ppm corresponds to the proton peak of solvent deuterium chloroform.the proton peak of —CH_3 at 0.88 ppm, the proton peak of —CH_2 in the middle of alkyl chain at 1.25ppm, the proton peak of —CH_2—in the imidazoline ring at 1.61ppm and the proton peak of —CH_2— in the imidazoline ring at 2.29ppm. A proton peak of N^+—CH_2 is at 3.67ppm. The proton peak of —CH_2— in the branched chain is at 3.24ppm.

2.2 Electrochemical system

The main test system is electrochemical workstation. Three electrode device is adopted. Platinum electrode was used as auxiliary electrode (CE), saturated calomel electrode as reference electrode (RE) and pure copper electrode (d = 2.0 mm, puratronic, Alfa aesar, 99.999%) as working electrode (WE). Use 200 mesh, 600 mesh and 2000 mesh sandpaper to polish the electrode surface to make it smooth and flat. The effective area of the working electrode was 0.0314cm^2. During the test, the working electrode was put into the environmental corrosion medium without adding or adding different concentrations of corrosion inhibitor. The polarization scanning rate is 1mV / s, and the scanning voltage range is -1V ~ 1V. All potentials reported in this paper are referred to SCE

2.3 Quantum chemical calculation

The quantum chemical calculations were carried out by using Gaussian 09 program[17]. Geometry optimization, highest occupied molecular energy (E_{HOMO}) and lowest unoccupied molecular energy (E_{LUMO}) were performed at the B3LYP/6-31G(d) basis[18-19] without any symmetry constraint.

3. RESULTS AND DISCUSSION

3.1 Influence of pH

Fig. 4 shows the Tafel and EIS plots for the copper electrodes with and without GIS were obtained in 3.5% M NaCl solution (pH=5,7 and 9).The electrochemical parameters obtained by fitting polarization curves with extrapolation method are shown in Table 1.

Table 1. Electrochemical parameters and slow-release efficiency of polarization curves of pure copper electrode in NaCl solutions with pH=5,7 and 9 respectively.

pH	Inhibitors	$-E_{corr}$(V)	ba(mV dec^{-1})	-bc(mV dec^{-1})	i_{corr}(μA cm^{-2})	η%
5	Blank	0.228	30	18	1.87	
	LG	0.172	15	13	1.67	10.92
	MG	0.210	9	7	1.67	10.78
	PG	0.195	19	16	1.72	7.82
	SG	0.197	21	25	1.78	4.79
7	Blank	0.204	18	14	1.73	
	LG	0.169	16	19	0.50	71.15
	MG	0.172	9	12	0.51	71.01
	PG	0.177	10	14	0.69	60.15
	SG	0.181	18	21	0.71	59.18
9	Blank	0.161	8	12	1.45	
	LG	0.159	16	22	0.23	83.91
	MG	0.145	8	10	0.24	83.00
	PG	0.138	28	7	0.27	80.84
	SG	0.167	13	10	0.35	75.59

As shown in Table 1, in NaCl solution with pH=5, the inhibition efficiency increases from 4.79% to 10.92% with the decrease of carbon chain length. Similarly, in NaCl solution with pH=7, the inhibition efficiency increases from 59.18% to 71.15% with the shortening of carbon chain length. In NaCl solution with pH=9, the inhibition efficiency increased from 75.59% to 83.91% with the decrease of carbon chain length. At the same time, we can see that GIS with the same carbon chain length has better corrosion inhibition effect in weak alkaline solution. For example, with the increase of pH from 5 to 9, the inhibition efficiency of LG increased from 10.92% to 83.91%.

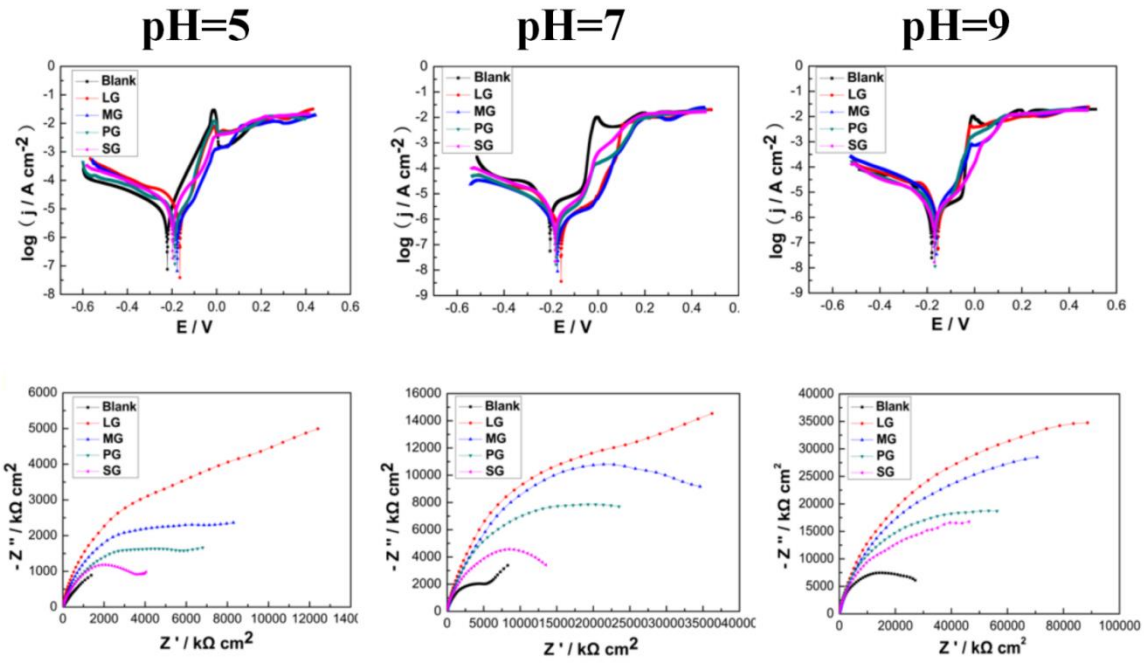

Figure 4. Polarization and impedance curves of GIS with carbon chain length and different pH of NaCl solution.

From Figure 4, we can see clearly that when four kinds of GIS with the same concentration are tested in NaCl solution with the same pH, the shorter the carbon chain length, the more positive the Tafel curve moves, and the higher the capacitance arc of EIS curve, the better the corrosion inhibition effect. Therefore, we can draw the conclusion that the inhibition effect of GIS is better in weak alkaline environment and shorter carbon chain length.

This is because the corrosion inhibition performance of organic corrosion inhibitors is closely related to their water solubility. Good water solubility of corrosion inhibitors is the prerequisite for their adsorption on the interface between metal and water solution. When the concentration of corrosion inhibitor is the same, the shorter the length of carbon chain, the better the water solubility, the more the adsorption amount of corrosion inhibitor on metal surface, the better the corrosion inhibition performance[20]. At the same time, the molecular structure is also an important factor affecting the corrosion inhibition performance. Because of the synergistic effect between short carbon chain molecules at the same concentration, the stable conformation with low energy can be formed and adsorbed on the metal surface to inhibit the corrosion reaction[21]. However, the long carbon chain corrosion inhibitors have a competitive relationship between carbon chains, which is characterized by high energy, unstable adsorption, and difficult to coordinate in the direction of molecule, so they are adsorbed on the surface of copper electrode.

3.2.1 Different concentration

The effects of imidazoline lauric acid Gemini surfactant concentration (50, 100, 150, 200 and 250mg/L) on its restrained effect were studied in NaCl solution with pH=9 and other conditions

unchanged. As shown in Fig. 5, with the increase of the concentration of imidazoline lauric acid Gemini surfactant in sodium chloride solution from 50 mg/L to 200 mg/L, the corrosion current density increases, the corrosion inhibition efficiency increases, and the curve moves in a positive direction. This indicates that LG is a corrosion inhibitor which mainly inhibits the anodic process. With the increase of LG concentration, the corrosion rate of copper electrode decreases and the slow-release efficiency increases. The higher sustained release efficiency is due to the adsorption of LG molecules on the surface of copper electrode.

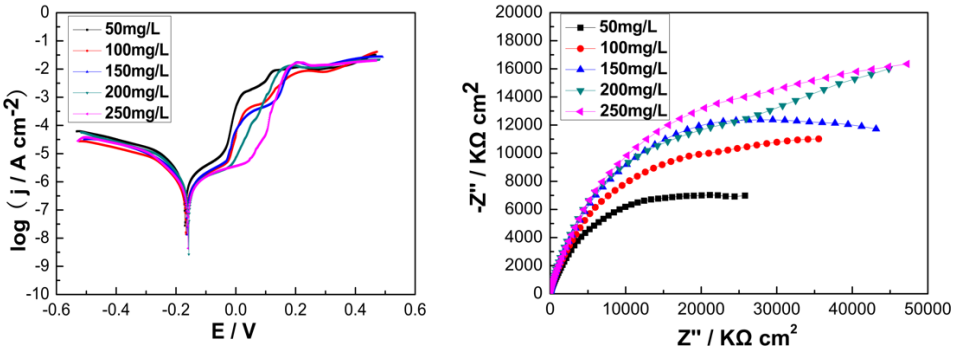

Figure 5. Polarization and impedance curves of GIS with different concentrations in NaCl solution

With the increase of inhibitor concentration, the slow-release efficiency increased rapidly, and then the component tended to be stable. When the concentration reached 250 mg/L, the sustained release efficiency decreased slightly, because LG was a good surfactant and there was a critical micelle concentration in NaCl solution. Under the critical micelle concentration, the inhibitor is mainly dispersed in the corrosive medium in the form of molecules. At this time, the adsorption amount of the inhibitor on the surface of the copper electrode increases with the increase of its mass fraction. When the mass fraction of the inhibitor reaches the critical micelle concentration, the mass fraction of the inhibitor in the presence of molecules will not increase with the increase of the amount of the inhibitor added, but will combine to form micelles. The amount of the inhibitor molecules adsorbed on the surface of the copper electrode will not increase significantly. Therefore, the slow-release efficiency of the inhibitor will not increase significantly. On the other hand, when the inhibitor reaches the critical micelle concentration, micelles are formed between the inhibitor molecules. Competitive adsorption between the inhibitor molecules adsorbed on the metal surface and the inhibitor micelles and water molecules will be elaborated, resulting in the phenomenon of "anodic desorption" of the inhibitor molecules adsorbed on the metal surface, resulting in a decrease in the slow-release performance[22]. The specific values are shown in Table 4.

It can be seen from Fig. 4 that the polarization curves of copper electrodes in NaCl solutions with different pH are composed of three potential regions: the formation of CuCl film and the diffusion process of $CuCl_2^-$ determine the Tafel region. As the potential increases gradually, the formation of CuCl film gradually dominates, and the potential gradually transits from the activation zone to the passivation

zone. When the CuCl film dissolves, the limit current region is formed on the surface of the electrode. The corrosion inhibition efficiency (η%) can be calculated by the formula.

$$\eta\,\% = \frac{i^{o}_{corr} - i_{corr}}{i^{o}_{corr}} \times 100$$

In this equation,i^{o}_{corr} and i_{corr} are the corrosion currents of the electrodes without and with GIS.The experimental parameters obtained in Fig. 4 and Fig. 5 are shown in Table 1 and Table 2. As the solution gradually changes from weak acidity to weak alkalinity, the concentration of the GIS increases, the length of carbon chain decreases, the corrosion inhibition rate increases, and the slow-release effect becomes better. which indicates that the self-assembled films of GIS formed are more compact and the coverage of the films on the electrode surface is higher[23,24].

Table 2. Electrochemical parameters and inhibitive effect efficiency of LG with different concentrations in NaCl solution at pH=9.

Inhibitors	C(mg /L)	$-E_{corr}$(V)	ba(mV dec^{-1})	-bc(mV dec^{-1})	i_{corr}(μA cm^{-2})	η%
LG	50	0.166	12	16	0.85	54.28
	100	0.171	8	11	0.54	68.65
	150	0.166	9	15	0.43	70.04
	200	0.159	16	22	0.23	83.91
	250	0.161	12	14	0.34	74.87

Impedance experiments show that the real and imaginary parts covered with SAMs are higher than those covered with blank copper electrodes, which means that the reactive resistance is higher and the capacitance value is smaller. In addition, the variation of self-corrosion potential and self-corrosion current of polarization curve is consistent with that of impedance. The above results show that the GIS on the surface of copper sample as a physical barrier prevents chloride ions from attacking copper electrode and reduces the diffusion rate of corrosion products, so the corrosion process is inhibited.

3.3 Quantum chemical calculations of GIS on copper electrodes surface

As we all know, ΔE, the difference between the E_{LUMO} and E_{HOMO}, is usually used to predict adsorption centers and corrosion inhibition efficiency of the inhibitors on metal surface. In the frontier orbital theory, the ability of the electron transition from HOMO to the potential acceptor increases with the value of E_{HOMO}, and the value of E_{LUMO} shows strength of the capability of accepting electrons for the LUMO. So, the higher values of ΔE means that the molecules have a good stability and lower reactivity. And the lower values of ΔE indicates that the the molecules have the better reactivity. Thus, in order to research the different inhibition process of LG, MG, PG and SG, the frontier orbitals of LG, MG, PG and SG were obtained by using Gaussian 09 program at the B3LYP/6-31G(d) basis, as shown in Table 3.

Table 3. Frontier orbital energies of GIS

Surfactants	E_{LUMO}/eV	E_{HOMO}/eV	ΔE/eV
LG	-0.25681	-0.37474	0.11793
MG	-0.25671	-0.36159	0.10488
PG	-0.25659	-0.35097	0.09438
SG	-0.25652	-0.34280	0.08628

From the Table 3, we can clearly see that both of the E_{HOMO} and E_{LUMO} for GIS decrease with shorter carbon chain. For example, the values of the E_{HOMO} and E_{LUMO} for SG is -0.25652 and -0.34280 eV, while that of for LG is -0.25681 and -0.37474 eV, respectively. It is indicates that the GIS with shorter carbon chain can acts as the potential electron acceptor, and the GIS with longer carbon chain can acts as the electron donor. As shown in Fig.6, it can be seen that the HOMO are spread over the alkyl chain, and the LUMO are mainly distributed in imidazole ring. It is noted that the ΔE values of GIS with longer (shorter) carbon chain is less than that of the GIS with shorter (longer) carbon chain, meaning that the GIS with shorter carbon chain owns the higher reaction activity, the stronger interaction with Cu and the higher protective efficiency than the GIS with longer carbon chain.

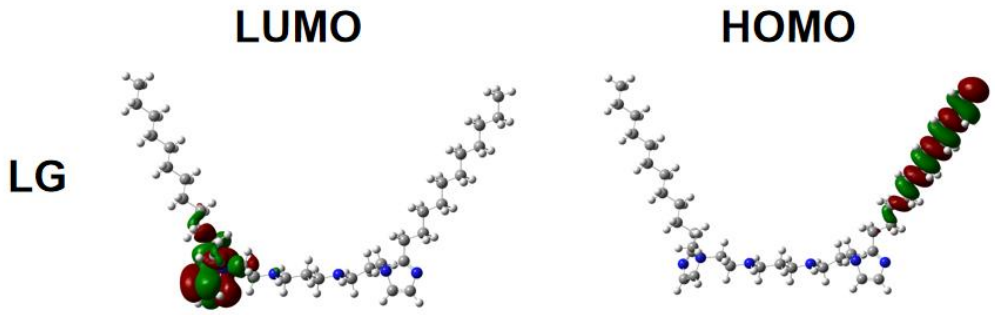

Figure 6. Electron distribution in the HOMO and LUMO for LG.

As described above, the distribution of the HOMO and LUMO can form multi-adsorption centers for the adsorption of GIS on the copper electrodes surface. On the one side, the nitrogen atoms of the imidazole ring can easy accept (provide) electrons to LUMO form the outer electrons of $4s^1$ of Cu atom. The occupied 4s orbital of Cu interact with the LUMO orbital of GIS forming a feedback bond. On the other side, the electron can be facilitates transferred to the vacant 4s orbitals of Cu from the HOMO, forming a coordination bond. The coordination bond and feedback bond forming between GIS and Cu atom enhances the adsorption stability of surfactant molecules on the Cu surface.

4. CONCLUSION

As a new surfactant, the research of GIS is in the ascendant. However, there are still few reports about the effect of its structure on its related performance. Our group is currently working on the effect of its structure on its performance. A series of GIS surfactants with different carbon chain lengths have

been synthesized and explored. Through comprehensive modification test, corrosion inhibition performance evaluation test and corrosion inhibition mechanism exploration test, the results are as described in this paper, and the following conclusions are drawn：

(1) With other conditions unchanged, GIS has a good inhibition effect in weak alkaline environment.

(2) When other conditions remain unchanged, the carbon chain length of GIS also affects its inhibitive effect. The shorter the carbon chain length, the better the suppressive effect. The higher the concentration of Gemini imidazoline inhibitor, the better the inhibition effect.

(3) When other conditions remain unchanged, increasing the concentration of corrosion inhibitor to a critical range can improve the coverage of corrosion inhibitor on metal surface and effectively protect metal.

ACKNOWLEDGEMENTS
This work received support from the National Natural Science Foundation of China (21703194) and the Special Fund for Promoting Scientific and Technological Innovation of Xuzhou (KC17080). An amount of computing time from Shandong University is also acknowledged.

References

1. F. Xu, Q. Zhang and Z.N. Gao, *Colloids Surf. A.*, 417 (2013) 201.
2. R. Fuchs-Godec, *Colloids Surf. A.*, 280 (2006) 130.
3. Z.Y. Fan, D.D. Li, X. Yu, Y.P. Zhang, Y. Cai, J.J. Jin, and J.H. Yu, *Chem. Eur. J.*, 22 (2016)3681.
4. L. Casal-Dujat, M. Rodrigues, A. Yague, A.C. Calpena, D.B. Amabilino, J. Gonzalez-Linares, M. Borras, and L. Perez-García, *Langmuir*, 28 (2912) 2368.
5. W.T. Wang, Y.C. Han, M.Z. Tian, Y.X. Fan, Y.Q. Tang, M.Y. Gao, and Y.L. Wang, *ACS Appl. Mater. Interfaces.*, 5 (2013) 5709.
6. M. A. Migahed, M. M. EL-Rabiei, H. Nady, H. M. Gomaa and E. G. Zaki, *J. Bio. Tribo. Corros.*, 3 (2017) 22.
7. T. Rasmussen, P. Sauerberg, E.B. Nielsen, M.D.B. Swedberg, C. Thomsen , M.J. Sheardown, L. Jeppesen, D.O. Calligaro, N.W. DeLapp, C. Whitesitt, J.S. Ward, H.E. Shannon, F.P. Bymaster and A. Fink-Jensen, *Eur. J. Pharmacol.*, 402 (2000) 241.
8. F.G. Liu, M. Du , J. Zhang and M. Qiu, *Corros. Sci.*, 51 (2009) 102.
9. L.W. Feng, C.X. Yin, H.L. Zhang, Y.F. Li, X.H. Song, Q.B Chen and H.L. Liu, *ACS Omega*, 3 (2018) 18990.
10. M. A. Migahed, M. M. EL-Rabiei, H. Nady, H. M. Gomaa and E. G. Zaki, *J Bio Tribo Corros.*, 3 (2017) 22.
11. X.M. Wang, H.Y. Yang, F.H. Wang, *Corros. Sci.*,52 (2010) 1268.
12. A. Teo, A. Mishra, I. Park, Y.J. Kim, W.T. Park and Y.J. Yoon, *ACS Biomater. Sci. Eng.*, 72 (2016) 472.
13. H. Wang, J. Liu, G. Gao, X. Wu, X.M Wang and H. Yang, *Brain Res.*, 7 (2015) 44370.
14. A. Khatory, F. Lequeux, F. Kern and S. J. Candau, *Langmuir*, 9 (1993) 1456.
15. D. Tripathy, A. Mishra, J. Clark and T. Farm, *C. R. Chimie.*, 24(2017) 1.
16. G. Gece, *Corros. Sci.*, 50 (2008) 2981.
17. N.L.P.A. Demorais and C.M.A. Brett, *J. Appl. Electrochem.*, 32 (2002) 653.
18. A. Edwards, C. Osborne, S. Webster, D. Klenerman, M. Joseph, P. Ostovar and M. Doyle, *Corros. Sci.*, 36 (1994) 315.

19. T. Zhou, J. Yuan, Y.J. Chen, X. Xin, Y.B. Tan and G.Y. Xu, *J. Surfact Deterg.*, 20 (2017) 529.
20. X.L. Wu, Y.P. Chu, Y.P. Huang, Z.C. Xu, L. Zhang, L. Zhang and S. Zhao, *J. Dispersion Sci. Technol.*, 01932691 (2016) 1140057.
21. S.P.R. Kobaku, C.S. Snyder, R.G. Karunakaran, G. Kwon, P. Wong, A. Tuteja and G. Mehta, *ACS Macro Lett.*, 8 (2019) 1491。
22. M. Mobin, R. Aslam and J. Aslam, Mater. *Chem. Phys.*, 191 (2017) 151.
23. Farelas F and Ramirez A, *Int. J. Electrochem. Sci.*, 5 (2010) 797.
24. M.A. Hegazy , M. Abdallah, M. Alfakeer and H. Ahmed, *Int. J. Electrochem. Sci.*, 13 (2018) 6824.